PHYSICAL REVIEW B **66**, 060503(R) (2002)

V-I characteristics in the vicinity of the order-disorder transition in vortex matter

Y. Paltiel,[1] Y. Myasoedov,[1] E. Zeldov,[1] G. Jung,[1,2,*] M. L. Rappaport,[1] D. E. Feldman,[1,†] M. J. Higgins,[3] and S. Bhattacharya[3,4]

[1]*Department of Condensed Matter Physics, Weizmann Institute of Science, Rehovot 76100, Israel*

[2]*Department of Physics, Ben-Gurion University of the Negev, Beer-Sheva 84105, Israel*

[3]*NEC Research Institute, 4 Independence Way, Princeton, New Jersey 08540*

[4]*Tata Institute of Fundamental Research, Mumbai-400005, India*

(Received 16 June 2002; published 8 August 2002)

The shape of the *V-I* characteristics leading to a peak in the differential resistance $r_d = dV/dI$ in the vicinity of the order-disorder transition in $NbSe_2$ is investigated. r_d is large when measured by dc current. However, for a small I_{ac} on a dc bias, r_d *decreases* rapidly with frequency, even at a few hertz, and displays a large out-of-phase signal. In contrast, the ac response *increases* with frequency in the absence of dc bias. These surprisingly opposite phenomena and the peak in r_d are shown to result from a dynamic coexistence of two vortex matter phases rather than from the commonly assumed plastic depinning.

DOI: 10.1103/PhysRevB.66.060503 PACS number(s): 74.60.Ge, 74.60.Ec, 74.60.Jg

Measurement of *V-I* characteristics or of the differential resistance $r_d = dV/dI$ in superconductors is a very common method to investigate vortex dynamics and to identify various possible pinned and moving phases of the vortex matter. In particular, the specific shape of *V-I* that leads to a peak in dV/dI has attracted much attention.[1–11] In numerical simulations this peak in r_d is usually ascribed to plastic vortex depinning followed by dynamic ordering of the lattice.[8–11] However, magnetic decorations and small-angle neutron scattering studies, which have observed the plastic deformation of the lattice near the depinning followed by the dynamic ordering,[12–14] did not find the predicted peak in dV/dI.[12,13] In addition, in clean systems such as $NbSe_2$ the peak in dV/dI is present surprisingly only in the lower part of the peak effect (PE), whereas in the rest of the *H-T* phase diagram the *V-I* curves are concave upward with no peak in dV/dI.[2,3,15] Moreover, in the same region where the peak in r_d is observed, a number of anomalous vortex matter properties were recently found, including the striking observation that for an ac current the apparent vortex mobility *increases* rapidly with frequency.[16–20] Several ideas and models have been proposed in which the ac agitation facilitates the plastic vortex depinning. Yet another important paradox has received little attention: when the ac current is superposed on a dc bias the opposite behavior is observed, i.e., the apparent vortex mobility *decreases* with frequency, even at frequencies as low as several hertz.[3] None of the models that describe the peak in r_d or the mobility enhancement with frequency[8–11,16] have resolved this apparent paradox.

In this paper we demonstrate that the shape of the *V-I* curves, the peak in dV/dI, and the opposite frequency dependencies stem, instead, from a dynamic coexistence of two vortex matter phases. A highly pinned metastable disordered phase (DP), generated at the sample edges, anneals into a weakly pinned equilibrium ordered phase (OP) in the bulk of the sample.[17,21,22] The specific shape of the dc *V-I* curves results from the fact that most of the sample is in the metastable DP at low currents, but in the OP at high currents. This dynamic transformation results in a peak in dV/dI. If measured by a small ac current superposed on a dc bias, we find that the peak in dV/dI decreases with frequency and displays a unique out-of-phase signal due to the slow transformation process. In contrast, for an ac current with no dc bias, only the edges of the sample are contaminated by the DP, resulting in the opposite behavior, i.e., the voltage response grows with the ac frequency.

Transport measurements were carried out on several Fe-doped (200 ppm) $NbSe_2$ crystals in striplike four-probe configuration in applied field *H* parallel to the c axis. The data presented here are for a $2\times0.4\times0.04$ mm^3 crystal with $T_c = 5.6$ K, $H_{c2}(4.2\text{ K}) = 1$ T, and the PE field $H_p(4.2\text{ K}) = 0.53$ T. Very low contact resistance of ~ 10 mΩ was achieved with large current contacts of Au evaporated onto a freshly cleaved surface. By immersing the crystals in liquid He, currents up to 100 mA could be applied with negligible heating. Square wave or sinusoidal I_{ac} was used and the corresponding V_{ac} was measured by a lock-in amplifier.

Figure 1 shows V_{ac} vs I_{ac} and V_{dc} vs I_{dc} in the vicinity of the order-disorder transition in the lower part of the PE at $H = 0.44$ T. The dc curve (solid circles) starts to increase in a *concave* form above 18 mA and then rapidly turns *convex*. At higher currents linear flux-flow behavior is obtained. Although the form of the dc *V-I* curve may seem rather conventional, we find that in $NbSe_2$ the convex shape is present

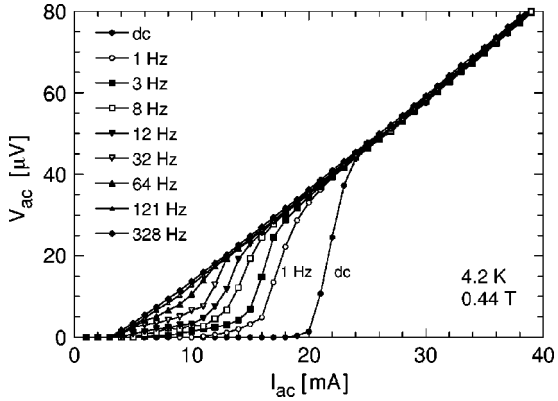

FIG. 1. V_{ac}-I_{ac} characteristics at various frequencies and V_{dc}-I_{dc} (●). The voltage response increases with ac frequency.

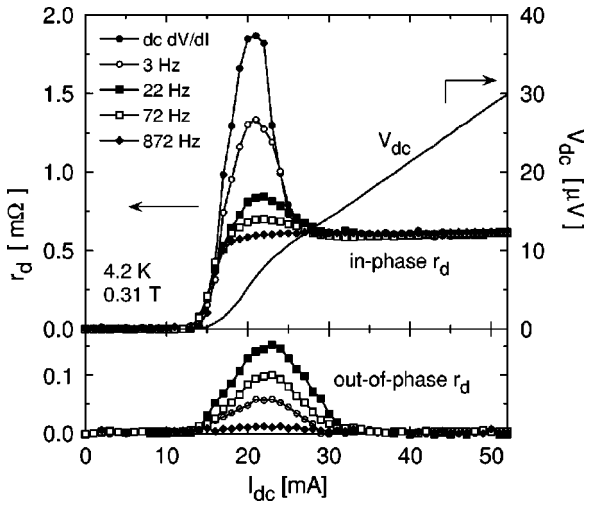

FIG. 2. In-phase and out-of-phase differential resistance r_d at dc (●) and various ac frequencies (left axis), and dc *V-I* characteristic (right axis). In-phase r_d decreases with frequency, while the out-of-phase r_d is maximal at intermediate frequencies.

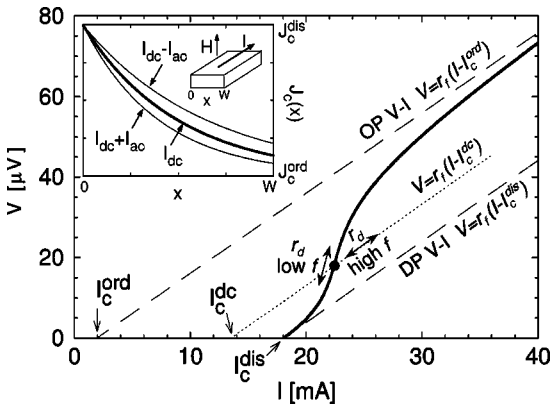

FIG. 3. Theoretical dc *V-I* characteristic (solid line) with $I_c^{ord}=2$ mA, $I_c^{dis}=18$ mA, $r_f=2$ mΩ, $W=400$ μm, and $L_r(V)=L_0(V_0/V)^{\eta}$ with $\eta=2$, $L_0=200$ μm, and $V_0=30$ μV. The frequency dependence of the differential resistance at the operating point (●) is shown in Fig. 4(b). Inset: Schematic sample geometry and $J_c(x)$ across the sample width. $J_c(x)$ decreases with increasing current.

only in the lower part of the PE, while in the rest of the phase diagram the curves are always concave upward, consistent with previous reports.[2,3,15] V_{ac} vs I_{ac} measured at various frequencies in Fig. 1 are remarkably different from the dc *V-I*. Even at a frequency as low as 1 Hz the apparent I_c is much lower and the voltage response below 20 mA is strongly enhanced. Furthermore, the apparent vortex mobility increases rapidly with frequency, as noted previously.[16–18]

Figure 2 shows the differential resistance r_d measured by superimposing a small I_{ac} (0.1 to 1 mA) on I_{dc}, $r_d=V_{ac}/I_{ac}$, along with $r_d=dV/dI$ obtained by numerical differentiation of the dc *V-I* at $H=0.31$ T. At this slightly lower field within the PE the dc *V-I* characteristic (solid curve) is more gradual and turns convex above ~20 mA. At the inflection point, dV/dI displays a large peak reaching three times the flux flow r_f. The remarkable result here is that the ac r_d is significantly different from the dc value[3] and it decreases rapidly with frequency. Note that the peak in ac r_d is suppressed to about half of the dc value already at f as low as 3 Hz, indicating the existence of very long characteristic time scales that are even longer than the vortex transit time across the sample, as described below. None of the microscopic bulk mechanisms, such as plastic depinning or dynamic ordering, can account for such long time scales. Moreover, due to the high sensitivity of the lock-in technique, the ac r_d vs I_{dc} is commonly integrated to derive the full *V-I* characteristics.[4,5] The important conclusion from Fig. 2 is that the integral of the ac r_d is *not equal* to the dc *V-I*.

Figures 1 and 2 display a striking qualitative difference: for a pure I_{ac} the measured V_{ac} *increases* with frequency, whereas for a small I_{ac} superposed on a larger I_{dc} the resulting V_{ac} *decreases* with f. The lower panel of Fig. 2 shows another puzzling aspect of the data, which is a large out-of-phase component that appears only in the nonlinear part of the *V-I* and is absent in the flux-flow region. An out-of-phase signal is a common feature in ac susceptibility measurements, where the amplitude of the current induced in the sample and the dissipation level depend on the excitation frequency. In transport measurements, in contrast, the amplitude of the current is fixed by the external circuitry and therefore the voltage response, as a rule, is frequency independent and does not show any out-of-phase signal at low frequencies. To the best of our knowledge this is the first published report of an imaginary r_d, which further emphasizes the anomalous vortex dynamics in the lower part of the PE. Note that the out-of-phase r_d is nonmonotonic with frequency: it vanishes in the limit of high and low f and is largest for the 22-Hz data.

We now discuss the results in view of the recent understanding that the PE reflects a disorder-driven first-order phase transition from a weakly pinned OP (Bragg glass) with a low critical current density J_c^{ord} into a strongly pinned DP with a high J_c^{dis}.[23–25] Local measurements have demonstrated that below the transition, in the lower part of the PE, in the presence of transport current a supercooled metastable DP is formed at the sample edge because of nonuniform vortex penetration through the surface barriers.[17,21,22] As the vortex lattice moves across the sample, the metastable DP with a high concentration of dislocations gradually anneals into the dislocation-free OP. We describe the annealing stage of the DP by its local critical current density $J_c(x)$, which has a nonequilibrium excess value $\tilde{J}_c(x)=J_c(x)-J_c^{ord}$ relative to the fully annealed OP. Since in low-temperature superconductors thermal activation is negligible, the sole annealing mechanism of the metastable DP is through a current-driven displacement that allows rearrangement and disentanglement of the vortices during the motion. We therefore assume, for simplicity, that the relative annealing of $\tilde{J}_c$ upon displacement by a small Δx is given by $\Delta x/L_r$, where L_r is a characteristic relaxation length over which the DP anneals into the OP. Since the lattice flows with velocity v, $\tilde{J}_c$ at $x+\Delta x$ and at time $t+\Delta t=t+\Delta x/v$ is thus described by $\tilde{J}_c(x+\Delta x,t+\Delta x/v)=\tilde{J}_c(x,t)(1-\Delta x/L_r)$, which leads to the partial differential equation of the annealing process

$$\partial \tilde{J}_c(x,t)/\partial x + (1/v)\partial \tilde{J}_c(x,t)/\partial t = -\tilde{J}_c(x,t)/L_r(v), \quad (1)$$

with a boundary condition at $x=0$, where vortices penetrate into the sample, of $\tilde{J}_c(0,t)=J_c^{dis}-J_c^{ord}$. A key aspect of the annealing process is that the relaxation length L_r crucially depends on the displacement velocity v. Fast transient measurements[26] show that at low velocities L_r is large, whereas for a potential landscape that is strongly tilted by a large driving force the disentanglement is very rapid, so that empirically $L_r \simeq L_0(v_0/v)^{\eta}=L_0(V_0/V)^{\eta}$. Here η is typically in the range of 1–3, L_0, v_0, and V_0 are scaling parameters, $V=vBl$ is the measured voltage drop, B is the magnetic field, and l is the distance between the voltage contacts. We now demonstrate that these simple assumptions describe all the essential experimental observations.

We first analyze the time-independent behavior. The dc solution of Eq. (1) is $J_c^{dc}(x)=(J_c^{dis}-J_c^{ord})\exp(-x/L_r)+J_c^{ord}$, as shown schematically in the inset of Fig. 3. By integrating over the width W we obtain the total critical current of the sample $I_c=d\int_0^W J_c^{dc}(x)dx$:

$$I_c(L_r)=(J_c^{dis}-J_c^{ord})[1-e^{-W/L_r(V)}]L_r(V)d+I_c^{ord}, \quad (2)$$

where $I_c^{ord}=J_c^{ord}Wd$ and d is the sample thickness. Note that I_c depends on L_r, which in turn depends on voltage V. This property is central to the described phenomena: Coexistence of the DP and OP results in an inhomogeneous sample and, moreover, the degree of the inhomogeneity, $J_c(x)$, changes with vortex velocity. As a result, the total I_c of the sample is not fixed, but rather changes with voltage.

The dc *V-I* characteristics can be derived as following. We write for simplicity the *V-I* of the OP as $V=r_f(I-I_c^{ord})$, where r_f is the flux-flow resistance. Similarly, when the entire sample is in the DP, $V=r_f(I-I_c^{dis})$ with $I_c^{dis}=J_c^{dis}Wd$. These two asymptotic *V-I* solutions are shown by the dashed lines in Fig. 3. Here we have assumed for simplicity that the flux-flow resistance r_f is the same for any of the phases. As a result, when the two phases coexist, $V=r_f(I-I_c)$, where I_c is given by Eq. (2) and is voltage dependent through $L_r(V)$. Hence an analytical $I(V)$ relation can be written directly as $I=V/r_f+I_c(L_r(V))$, and the resulting nonlinear *V-I* characteristic is shown by the solid curve in Fig. 3. At very low voltages L_r is larger than the sample width, namely, the entire sample is contaminated by the DP, and hence the *V-I* initially follows the asymptotic dashed line of the DP with $I_c=I_c^{dis}$. At high vortex velocities L_r becomes very short, most of the sample is in the OP, and the *V-I* approaches the asymptotic line of the OP with $I_c=I_c^{ord}$. In the crossover region a specific shape of the curve with an inflection point is obtained alike the experimental dc *V-I* curves in Figs. 1 and 2. This shape is the result of a continuous decrease of the total I_c of the sample from $I_c=I_c^{dis}$ to $I_c=I_c^{ord}$ with increasing current. The exact curvature in the crossover region depends on the parameters η, L_0, and V_0 (see Fig. 3 caption) and may be either gradual or very steep, and may even obtain a negative slope resulting in an S-shaped characteristic as found recently in the lower part of the PE.[27]

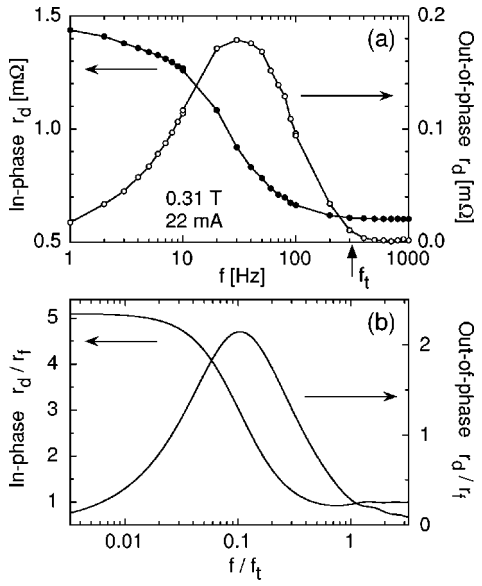

FIG. 4. (a) Frequency dependence of the in-phase (●) and out-of-phase (○) r_d at $I_{dc}=22$ mA near the peak of r_d in Fig. 2. (b) Calculated r_d/r_f vs f/f_t at the operating point in Fig. 3.

In order to understand the frequency dependence of the differential resistance shown in Fig. 2 and in more detail in Fig. 4(a), we solve Eq. (1) for a small periodic velocity perturbation $v=v_{dc}+v_{ac}e^{i\omega t}$ caused by applied current $I_{dc}+I_{ac}e^{i\omega t}$. In this case $L_r(v)=L_{dc}+(dL_r/dv)v_{ac}e^{i\omega t}$. Following a simple calculation and keeping only the linear terms in v_{ac}, we obtain $J_c(x,t)=J_c^{dc}(x)+J_c^{ac}(x)e^{i\omega t}$, where $J_c^{ac}(x)=(J_c^{dis}-J_c^{ord})(dL_r/dv)(v_{dc}v_{ac}/L_{dc}^2)e^{-x/L_{dc}}(1-e^{-i\omega x/v_{dc}})/i\omega$. Note that $J_c^{ac}(x)$ is negative because of a negative dL_r/dv, reflecting the fact that the system becomes more ordered with increasing v. In the limit of low frequency, $J_c(x,t)$ slowly varies between two extreme dc solutions determined by $L_{dc}\pm(dL_r/dv)v_{ac}$, as shown in the inset of Fig. 3. At the minimum value of the current, $I_{dc}-I_{ac}$, the vortex velocity is lowest, L_r is largest, and hence $J_c(x)$ is highest. At the maximum of the current, $I_{dc}+I_{ac}$, L_r is smallest and the sample is "cleanest," resulting in a large enhancement in the vortex velocity. Hence the large r_d at low f arises from the varying contamination of the sample, which significantly amplifies the voltage response. However, modification of the sample contamination is a slow process because the only mechanism of enhancement of the local disorder in the bulk is by transporting a more disordered lattice from the edge of the sample. This results in characteristic time scales comparable with the vortex transit time across the sample $\tau_t=W/v$ (or even longer, see below).

To obtain the full frequency dependence of r_d we calculate $I_c^{ac}=d\int_0^W J_c^{ac}(x)dx$, and by noting that $V_{ac}=r_f(I_{ac}-I_c^{ac})$, we find $r_d=V_{ac}/I_{ac}=(1/r_f+I_c^{ac}/V_{ac})^{-1}$. This result shows that the enhancement of r_d results from the fact that I_c^{ac} is negative, and depending on the $L_r(v)$ parameters, r_d can become infinite and even negative for the case of S-shaped *V-I* curves. The full analytical expression for r_d is too extensive to be presented here. Figure 4(b) therefore shows the calculated real and imaginary parts of r_d/r_f vs

frequency at the operating point in Fig. 3. At low frequencies, the in-phase r_d is large and it decreases towards r_f when f approaches the transit frequency $f_t = 1/\tau_t$. We can understand this behavior as follows. As indicated by the arrows in Fig. 3, at low frequencies r_d is given by dV/dI, which can be very large depending on the specific shape of the dc V-I curve. However, the surprising result here is that at higher frequencies, in contrast to the common belief, the experimental $r_d = V_{ac}/I_{ac}$ does not measure the true dV/dI. At high f the local degree of disorder $J_c(x,t)$ cannot adjust to the rapid variations and therefore $J_c(x,t)$ is fixed at $J_c^{dc}(x)$, and $J_c^{ac}(x)$ and I_c^{ac} vanish. As a result, at high frequency the ac signal, instead of following the dc curve, follows a trajectory shown by the dotted line in Fig. 3. This line is the V-I characteristic of a sample with a fixed $I_c = I_c^{dc}$, $V = r_f(I - I_c^{dc})$, resulting in $r_d = r_f$, as indeed observed experimentally in Figs. 2 and 4(a).

The rearrangement of the bulk disorder always lags the external ac drive, giving rise to a pronounced imaginary r_d component [Fig. 4(b)] that has a maximum at intermediate frequencies. The qualitative agreement between the results of our simplified calculations in Fig. 4(b) and the experimental data in Fig. 4(a) is remarkable, including the frequency scale: The experimental transit frequency $f_t = V_{dc}/BWl$, marked by the arrow in Fig. 4(a), was obtained by a direct measurement of V_{dc}, and the maximum of the out-of-phase r_d occurs at about $0.1 f_t$, in excellent agreement with the calculated behavior.[28]

Finally, we comment briefly on the response to a large I_{ac} with no I_{dc} as shown in Fig. 1. In contrast to the previous situation, here all the metastable DP exits and reenters the sample during every ac cycle, as shown previously.[17] The detailed analysis of this case is much more complicated since $J_c(x,t)$ changes significantly during the ac cycle and is different for the entering and exiting edges, resulting in highly nonlinear behavior that cannot be treated analytically. Qualitatively, however, the maximum depth to which the DP penetrates the sample from each edge during the corresponding half period of the ac cycle is $x_d^{ac} = v/2f$, where v is the average vortex velocity during the half cycle, while the central part of the sample remains ordered. Therefore the fraction of the sample occupied by the DP decreases with f as $x_d^{ac}/W \propto 1/f$. Consequently, the volume of the OP increases with frequency, the integrated I_c decreases, and V_{ac} increases. At sufficiently high f, practically the entire sample becomes ordered so that the experimental V_{ac}-I_{ac} in Fig. 1 follows the asymptotic dashed OP curve in Fig. 3. Thus a high-frequency measurement of V_{ac}-I_{ac} is a useful method to reduce edge contamination and to approximate the true V-I of the OP.

In summary, the process of edge contamination by the metastable disordered phase in the vicinity of the order-disorder transition is shown to explain the convex shape of the V-I characteristics in the lower part of the PE, the large difference between V_{dc}-I_{dc} and V_{ac}-I_{ac} curves that grows with frequency, the peak in the differential resistance and its rapid suppression with frequency, the out-of-phase signal in ac transport measurements, and the opposite frequency dependence in the different cases of ac drive.

This work was supported by the Israel Science Foundation - Center of Excellence Program and by the Minerva Foundation, Germany. E.Z. acknowledges support by the Fundacion Antorchas - WIS Collaboration Program, and D.E.F. acknowledges support by RFBR Grant No. 00-02-17763 and by the U.S. DOE, Office of Science, Contract No. W31-109-ENG-38.

*Also at Instytut Fizyki PAN, Warszawa, Poland.

†Present address: Argonne National Laboratory, Argonne, IL 60439 and Landau Institute for Theoretical Physics, Chernogolovka 142432, Russia.

[1] R. Wordenweber and P.H. Kes, Phys. Rev. B **34**, 494 (1986).

[2] S. Bhattacharya and M.J. Higgins, Phys. Rev. Lett. **70**, 2617 (1993).

[3] S. Bhattacharya and M.J. Higgins, Phys. Rev. B **52**, 64 (1995); M.J. Higgins and S. Bhattacharya, Physica C **257**, 232 (1996).

[4] F. Garten, W.R. White, and M.R. Beasley, Phys. Rev. B **51**, 1318 (1995).

[5] M.C. Hellerqvist *et al.*, Phys. Rev. Lett. **76**, 4022 (1996).

[6] J.M.E. Geers *et al.*, Phys. Rev. B **63**, 094511 (2001).

[7] Z.L. Xiao *et al.*, Phys. Rev. Lett. **85**, 3265 (2000).

[8] A.E. Koshelev and V.M. Vinokur, Phys. Rev. Lett. **73**, 3580 (1994).

[9] S. Ryu *et al.*, Phys. Rev. Lett. **77**, 5114 (1996).

[10] C.J. Olson, C. Reichhardt, and F. Nori, Phys. Rev. Lett. **81**, 3757 (1998); A.B. Kolton, D. Dominguez, and N. Gronbech-Jensen, *ibid.* **83**, 3061 (1999).

[11] M.C. Marchetti, A.A. Middleton, and T. Prellberg, Phys. Rev. Lett. **85**, 1104 (2000).

[12] U. Yaron *et al.*, Nature (London) **376**, 753 (1995).

[13] A. Duarte *et al.*, Phys. Rev. B **53**, 11 336 (1996).

[14] F. Pardo *et al.*, Phys. Rev. Lett. **78**, 4633 (1997).

[15] Z.L. Xiao *et al.*, Phys. Rev. B **65**, 094511 (2002).

[16] W. Henderson, E.Y. Andrei, and M.J. Higgins, Phys. Rev. Lett. **81**, 2352 (1998).

[17] Y. Paltiel *et al.*, Nature (London) **403**, 398 (2000).

[18] V. Metlushko *et al.*, cond-mat/9804121(unpublished).

[19] S.N. Gordeev *et al.*, Nature (London) **385**, 324 (1997).

[20] W.K. Kwok *et al.*, Physica C **293**, 111 (1997).

[21] M. Marchevsky, M.J. Higgins, and S. Bhattacharya, Nature (London) **409**, 591 (2001); Phys. Rev. Lett. **88**, 087002 (2002).

[22] D. Giller *et al.*, Phys. Rev. Lett. **84**, 3698 (2000); C.J. van der Beek *et al.*, *ibid.* **84**, 4196 (2000).

[23] Y. Paltiel *et al.*, Phys. Rev. Lett. **85**, 3712 (2000).

[24] N. Avraham *et al.*, Nature (London) **411**, 451 (2001).

[25] G. Ravikumar *et al.*, Phys. Rev. B **63**, 024505 (2001).

[26] W. Henderson *et al.*, Phys. Rev. Lett. **77**, 2077 (1996).

[27] A.A. Zhukov *et al.*, Phys. Rev. B **61**, R886 (2000).

[28] Note that in Fig. 4 the characteristic timescale is ten times longer than the transit time. This is one of the interesting consequences of Eq. (2) and arises from the fact that for a full rearrangement of the $J_c(x)$ distribution from minimum to maximum (see Fig. 3 inset), the vortices have to cross the sample several times, depending on $L_r(v)$ and the operating point on the V-I curve.